

Semester Project Report

Construction of a Thermal Noise Source for the
Calibration of a Parametric Amplifier

Juan Osorio

Department of Physics

ETH Zürich

`juanos@student.ethz.ch`

Supervisor: Christopher Eichler

Contents

1	Introduction	1
2	Calibration Method	2
2.1	Y-factor measurement	3
3	Understanding Heat-Flow	5
3.1	Two basic questions	5
3.2	The Simulations	5
3.2.1	Simulation Parameters	7
3.2.2	The Heat Channel	8
3.2.3	Results	9
4	The Set-up	11
4.1	The Thermal Noise Source (TNS)	11
4.2	Electrical connections for the heater and the temperature sensor	12
4.3	The heater	12
5	The Experiment	13
5.1	Experimental Set-up	13
5.2	Results	16

5.3 Error Bars	18
6 Conclusions	20

1 Introduction

One of the main tools of present-day state-of-the-art research in the field of cQED, as well as quantum information processing using superconducting qubits, is the Josephson Parametric Amplifier (JPA). The wide variety of scenarios where these devices can be used spans single-qubit signal amplification, vacuum noise squeezing, as well as the detection of the position of nanomechanical oscillators with quantum-limited sensitivity, among others.

It is the goal of this document to report on the construction of a thermal noise source to be used for the calibration of a JPA at the Quantum Device Laboratory of Professor Andreas Wallraff at ETH Zürich.

2 Calibration Method

A well-known method for characterizing amplifiers is the so-called *Y-factor* measurement [1]. I will briefly explain what the procedure behind such a measurement is, for the case in which one wants to measure the noise temperature of a given amplifier.

The output power of an amplifier with constant gain G over some bandwidth B , can be written as:

$$P_{out} = G(P_{in} + P_{noise})$$

where P_{in} represents the input power of the signal and P_{noise} the noise power of the amplifier at its input. Now, one may define the noise power of an amplifier in terms of a *noise temperature* (a quantity independent of B), by means of the following expression:

$$P_{noise} = Bk_B T_{noise}$$

where T represents the noise temperature of the amplifier, and k_B the Boltzmann constant. Even though T_{noise} will be independent of our bandwidth, it need not coincide with its physical temperature (indeed, for a 1-D blackbody one can prove that $P = Bk_B T$ in a regime in which $k_B T \ll h\nu$, ν being the frequency being measured [1]).

This tells us that if we had precise knowledge of our amplifier's gain and could somehow manage to make the noise temperature go to zero for our input signal, we could automatically find out the noise temperature of our amplifier by simply relating it to the output power. Since this is not possible, one usually uses the so-called *Y-factor* measurement.

2.1 Y-factor measurement

Consider two situations analogous to the previous one, except that in each situation we will plug to the *in*-port of our amplifier a blackbody radiator at two different temperatures, T_0 and T_1 . If we do this, and express the powers in terms of the noise temperatures, what we find is:

$$\begin{aligned} P_{out}^0 &= BGk_B (T_0 + T_{noise}) \\ P_{out}^1 &= BGk_B (T_1 + T_{noise}). \end{aligned} \tag{1}$$

Notice that even though the noise temperature need not match the physical temperature of the device, there will indeed be a correlation between the two, i.e. the noise temperature and the gain of any amplifier need not be independent of its physical temperature. What this means in terms of the previous equations is that we have made the assumption that in performing our measurement we have managed to keep the physical temperature of the amplifier constant, so that we get identical noise contributions as well as gain figures from the amplifier on both measurements.

Furthermore, by taking the ratio of these equations and clearing out the variable T_{noise} what we find is

$$T_{noise} = \frac{T_1 - YT_0}{Y - 1}$$

with

$$Y = \frac{P_{out}^1}{P_{out}^0}.$$

Hence by defining a new parameter (namely the *Y-factor*) we can find a simple expression for the noise temperature of our amplifier, independent of the amplifier's gain, which amounts to performing two power spectrum measurements and taking the ratio of the results.

We can realize such a blackbody source using a 50Ω termination, which will have a blackbody-like radiation spectrum within the frequency regime between $3 - 8\text{GHz}$, which is our amplifier's bandwidth.

Since all our measurements will be performed inside the black Oxford Instruments cryostat, it is necessary to consider the effect that our experimental set-up will have on the operating temperature of the plate on which we will mount our equipment.

In the following section we will discuss this effect by simulating different possible scenarios and evaluating which one proves to be the most favorable one for our purpose.

For the sake of clarity a photo of our final configuration is included so that the reader can get a better feeling of how our set-up was arranged in the cryostat (See Fig. 1).

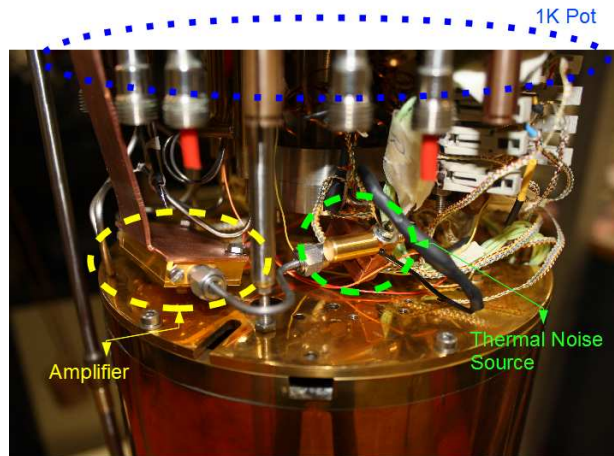


Figure 1: **Experimental Set-up.** *Final arrangement of our experimental set-up. The TNS was mounted directly on the input of the amplifier without any additional support. The amplifier itself was directly mounted on the 1K Pot by means of a copper holder. Special attention was paid to mounting both the amplifier as well as the TNS without contact to any other surfaces which could provide additional heat channels.*

3 Understanding Heat-Flow

3.1 Two basic questions

In order to get a better idea of the behaviour of the temperature of the set-up as we performed the Y-factor measurement, we needed to address two questions that were of key importance, namely:

- Is the TNS isolated enough from our amplifier, so that we do not change the physical temperature of the latter while manipulating the TNS temperature?
- If indeed the TNS is isolated enough from the rest of the set-up, will it cooldown from room temperature within a reasonable time?

In providing answers to these questions it was important to determine a good set of parameters that would allow one to carry out a simulation of the cooling down of the TNS, since it was desired to carry out the calibration of the amplifier without the need to wait for an unreasonable time (more than one week). The problem of balancing a reasonable cooldown time for the TNS with an unexcessive thermalization of the base plate turned out to be one of the main tasks of this project.

3.2 The Simulations

The simulations were done by simplifying the real problem, in which a complex geometry of the internal parts of the cryostat along with multiple heat flow channels play a role, to one where only two bodies exchange heat through some heat-exchange channel (coaxial cable) and one of them is in contact with the cryostat's cooling power.

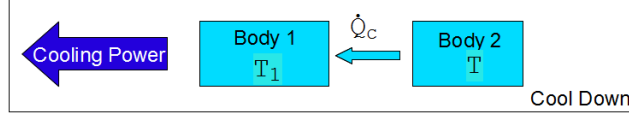


Figure 2: **Schematic of Cool Down.** *The cooling power of the cryostat drains heat from Body No. 1 (base plate), while Body No. 1 drains heat from Body No. 2 (TNS, Heater and Temp. sensor). Arrows represent heat flow between the elements.*

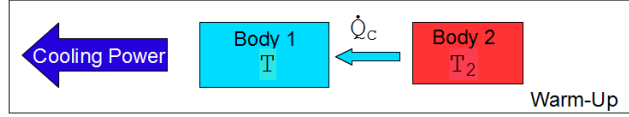


Figure 3: **Schematic of Warm-Up.** *The TNS is heated for the measurement and kept at a constant temperature T_2 . Heat is being drained from Body No. 1 by the cooling power of the cryostat while Body No. 2 transfers heat to Body No.1, generating a competition between heating and cooling powers.*

That is, the problem was one where the base plate (body #1) is coupled to the cooling power of the cryostat on one end and, on the other end, to the TNS (body #2) via a coaxial cable (the heat exchange channel) (the temperature sensor and the heater were also included in body #2, this approximation was made since the materials they are made of are very similar to those of the TNS). For a diagrammatic illustration see figures 2 and 3. Once this approximation had been done, the following equations were used to perform the simulations:

$$\frac{\partial Q_c}{\partial t} = \frac{A\lambda(T)}{L} \Delta T \quad (2)$$

$$\frac{\partial Q_e}{\partial t} = \frac{\partial T}{\partial t} C(T) \quad (3)$$

where A is the cross-sectional area of the coaxial cable, λ the heat conductivity of the coaxial cable, L the length of the cable, Q_c the heat flowing through the cable and Q_e the net heat transfer, the rest of the terms will depend on the scenario being simulated. For the cool down, T is the temperature of the TNS, ΔT is the temperature difference between the TNS

and the base plate, and C is the heat capacity of the TNS. In this scenario Q_c and Q_e will both be equal to the heat being drained from the TNS, hence the two equations can then be reduced to:

$$\frac{\partial T}{\partial t} = \frac{A\lambda(T)}{LC(T)}\Delta T$$

For the warm-up, T is the temperature of the base plate, ΔT is the temperature difference between the base plate and the TNS, C is the heat capacity of the base plate, Q_c the heat injected from the TNS to the base plate and Q_e is the net heat transfer to the base plate, i.e. $Q_e = Q_c - Q_{cp}$, with Q_{cp} the cooling power of the cryostat.

3.2.1 Simulation Parameters

The main parameters considered in these simulations were the following (materials being indicated in parentheses):

- Cooling power of cryostat.
- Heat capacities.
- Thermal conductivities.
- Mass of base plate (Brass).
- Length of coaxial cable.
- Mass of TNS (Mostly copper).
- Mass of heater (Copper).
- Mass of temperature sensor (Mostly copper).

The cooling power was obtained at low temperatures from vericold industries and estimated for higher temperatures [2]. Both the heat capacities and the thermal conductivities were extracted from available literature [7], the mass of the base plate was estimated by using a previous cooldown curve from one of the vericold cryostats (see Fig. 4), the masses of the TNS, the heater and the temperature sensor were calculated from the geometry of these components [2].

3.2.2 The Heat Channel

To measure the exact amount of noise that is being introduced by the amplifier one uses the previously mentioned TNS as a calibration device. In order to allow the radiation from the TNS to reach the amplifier without attenuation effects playing a significant role, a coaxial cable with very little electrical resistance (ideally none) is needed. Minimization of this uncertainty coming from attenuation effects is essential since it could lead to variations in the noise power estimation for the amplifier, this can be seen from Eq. 1. Since one of our main assumptions is that the temperature of the amplifier will remain constant while performing the measurement, it was of primary importance to find a material that would provide an excellent electrical conductivity as well as good thermal isolation properties. After reviewing a series of materials available [7], five types of cables were selected:

- Stainless Steel/Stainless Steel (Inner conductor/outer conductor).
- Stainless Steel/NbTi.
- CuNi/NbTi.
- NbTi/NbTi.
- YBCO/YBCO.

Where it is important to mention that NbTi becomes superconducting at $T_c = 9K$, as well as YBCO with $T_c = 93$, meaning that for these materials attenuation would be suppressed almost completely below their T_c .

3.2.3 Results

A comparison between a “calibration” simulation and a real cooldown can be seen in figure 4. This simulation was performed without including the TNS, so that by looking for a value of the mass of the base plate which reproduced the real data adequately we could obtain a reasonable estimate for its real value.

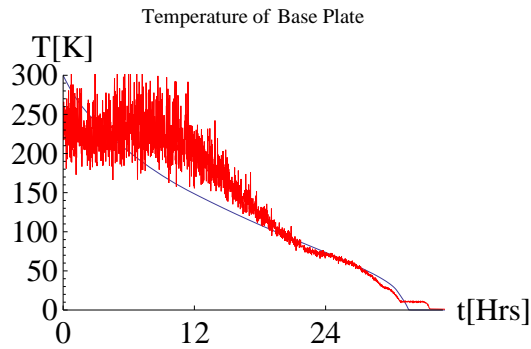


Figure 4: **Real Data vs Simulation.** Temperature vs Time plot comparing real data (red) and our simulation (blue) for the cool down scenario (since this simulation was used as a calibration, the TNS was not included). By comparing these two plots we managed to make a reasonable estimate of the mass of the base plate.

In figure 5, a comparison of the cooldown time for the TNS, using different materials for the coaxial cable, is shown.

These simulations provided a common ground on which the different materials could be compared under identical circumstances, hence giving an idea of their relative behavior.

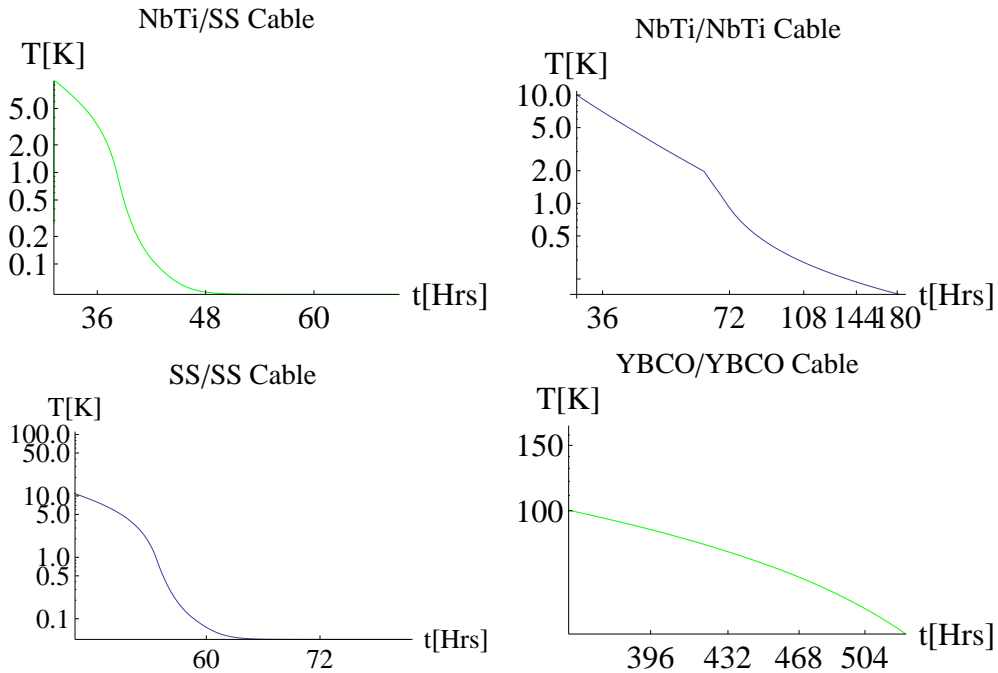


Figure 5: **TNS Cool down Plots.** Plots for the cool down using: YBCO, Stainless Steel, NbTi/SS and NbTi cables.

An excessive cooldown time for YBCO is indicated by the simulations, since after one week it did not seem to have reached 10K, on the other hand the SS/SS and NbTi/SS cables showed good thermal conductance so that after 3 days both had reached base temperature, finally a cable showing an intermediate cooldown time was NbTi/NbTi reaching base temperature after a week of cooling. These can be seen as reasonable results given the fact that, as is shown in figure 4, cooling the base plate down to base temperature requires approximately 36 hours.

Having discussed the cool down behavior of our system, we will now consider the situation in which the TNS is heated up and kept at some fixed temperature as was the case during our measurements, in order to get a better feeling of how the temperature of the base plate would behave under such a scenario. Figure 6 shows a comparison of the expected thermalization for the base plate for TNS temperatures of 4K and 8K during the 'warm' step of the calibration procedure, when using the different materials.

In the case of the TNS at 4K, it was found that the temperature of the base plate did not exceed 40mK with any material, whereas in the case of the TNS heated up to 8K the temperature reached a maximum of 100mK with the NbTi/CuNi cable. Taking these observations into account it was quite clear that the cable that provided the best balance was the NbTi/NbTi cable (see Mathematica notebook in [6]).

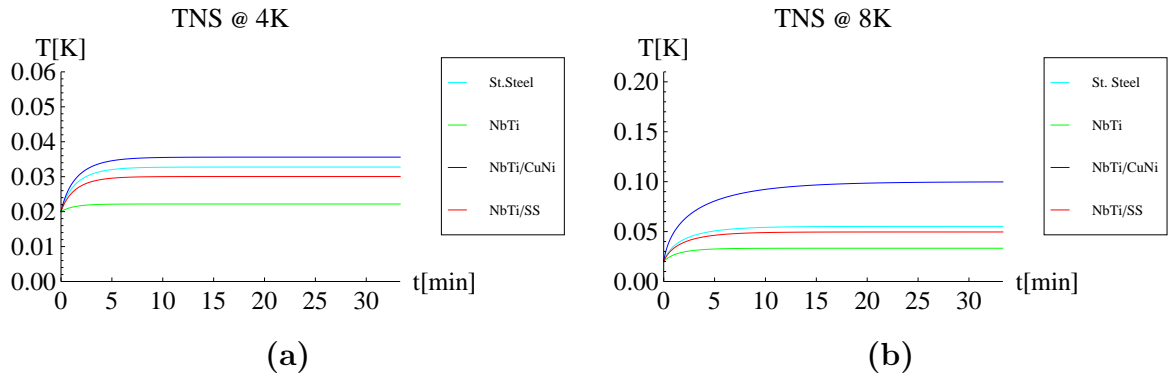


Figure 6: **Base Plate Thermalization.** *Temperature vs Time Plot for the thermalization of the base plate using four of the different materials considered when the TNS is operated at: (a) 4K and (b) 8K.*

4 The Set-up

4.1 The Thermal Noise Source (TNS)

A 50Ω male termination was used as noise source [2]. Since these terminations are designed to operate as close as possible to blackbodies absorbing radiation over the range of 0 to 20Ghz, it is also possible to use these terminations as blackbodies emitting a well known radiation spectrum. That is, by manipulating the temperature of the termination, emission of electromagnetic radiation close to that of a blackbody is obtained, allowing one to control precisely the radiation going into the amplifier and thus allowing one to use them for

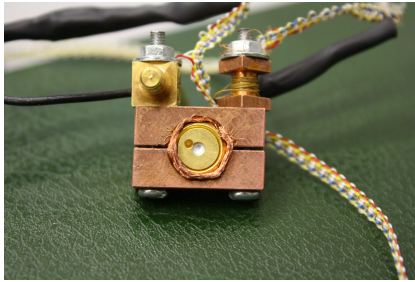


Figure 7: ***The Thermal Noise Source.*** The 50Ω termination (center) together with the heater (upper right) and the temperature sensor (upper left). A copper holder was used with some copper strand around the 50Ω termination to increase thermal contact.

calibration.

In our implementation we chose to control the temperature of the termination by means of a heater and a temperature sensor mounted directly on it. A picture of these components can be seen in figure 7 (for additional images of the set-up refer to my personal folder [3]).

4.2 Electrical connections for the heater and the temperature sensor

NbTi stranded-pair wires with a length of 100cm were used as electrical leads for the heater and the temperature sensor, this made heat flow from the TNS to the rest of the set-up through these wires negligible due the low heat conductivity of NbTi, as well as the reduced cross sectional area ($100\mu\text{m}$ diameter) and the length of the wire.

4.3 The heater

A silk-isolated constantan-wire winding was used to make a 9Ω resistor. Both the heater and the temperature sensor were controlled using a Lakeshore AC 370 resistance bridge. The total resistance was chosen to be 9Ω given the fact that the cooling power of the vericold

cryostat was estimated to be around 400mW at 4.2K, and since the maximum excitation current for the resistance bridge is 100mA, we could obtain around 90mW of heating power, which together with a poor thermal conductivity between the TNS and the rest of the set-up, was thought to provide enough heating power. It was observed that this heating power was indeed more than enough to allow a gentle manipulation of the temperature of the set-up without the need to use the maximum current setting in the resistance bridge.

5 The Experiment

For the experiment we used our TNS to measure the noise temperature of a HEMT amplifier (from here on referred to as “cold” amplifier) for which calibration data were available from the manufacturer. This allowed us to compare the available specifications with our measured results. All measurements were performed inside the black Oxford Instruments cryostat.

5.1 Experimental Set-up

The final length selected for the coaxial cable carrying the signal from the TNS to the cold amplifier was 7 cm given that the results from the simulations corresponding to this length proved adequate. Standard SMA crimp male connectors were used for both ends of the NbTi cable. An additional Stainless Steel coaxial cable with a length of 150cm was made in order to take the signal from the *out*-port of the cold amplifier to the top loading unit (TLU) of the cryostat. The signal was then read in an Agilent 4407B ESA Spectrum Analyser for which the noise floor was observed to be around -120dBm. The amplification figure for the cold amplifier was known to be 40dB over the entire bandwidth [2]. Two additional amplifiers (“warm” amplifiers) were required to obtain a power figure that could be measured given the observed noise floor of the spectrum analyzer. The first of these two additional amplifiers was placed right on the TLU to which the previously mentioned stainless steel cable was

connected directly, whereas the second amplifier was mounted directly on the in-port of the spectrum analyzer. The noise temperatures of these two amplifiers were 233K and 450K over the range of frequencies in which we were interested, and their corresponding amplification figures were 33dB and 27dB, respectively [2]. Standard SMA solder male connectors were used for the Stainless Steel cable. All cables used in the set-up were standard 0.085 in. diameter coaxial cables.

For the temperature measurements at the TNS a ruthenium oxide temperature sensor from Oxford Instruments was used, the calibration curve was saved in the resistance bridge under the name “ROX TEMPERATURE SENSOR”. The calibration curve for this sensor was given for temperatures below 4.2K; we used the same curve provided in the specifications sheet to extend these data up to 6K since this would be the temperature for the “warm” stage of the measurement.

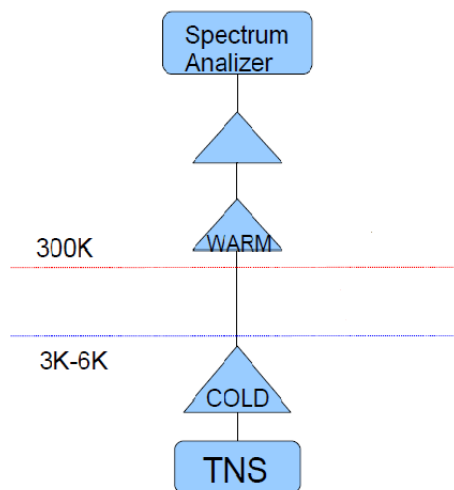


Figure 8: ***Schematic of Experimental Set-Up.*** Schematic illustration of the actual experiment. Our configuration consisted of 3 cascaded amplifiers with one stainless steel coaxial cable in between the cold amplifier and the first warm amplifier. The red and blue lines indicate the different temperature regions of the set-up.

The set-up used for the experiment is illustrated in figure 8, as can be seen, the TNS is

connected directly to the input of the amplifier. Attached to the TNS one can find both the heater and the temperature sensor.

Not shown in this schematic but present in the actual equipment are the leads in charge of connecting both the heater and the sensor to a resistance bridge outside the cryostat.

The fact that the cable carrying the signal from the cold amplifier to the top loading unit was chosen to be of stainless steel was based on the fact that these cables are the standard choice for such applications. This is done to minimize heat conductance through the cable, coming at the cost of relatively high attenuation figures.

It can be verified easily that this cascaded chain of amplifiers gives an expression for the noise temperature of the first amplifier of the chain, as follows:

$$T_c \approx \frac{T_{NS}^\uparrow - Y T_{NS}^\downarrow}{Y - 1} - \frac{T_w}{G_0 K_0} \quad (4)$$

where T_c stands for the noise temperature of the cold amplifier, T_{NS}^\uparrow and T_{NS}^\downarrow stand for the temperatures of the TNS during the 'warm' and 'cold' stages, T_w stands for the noise temperature of the warm amplifier mounted on the TLU, G_0 for the gain of the cold amplifier and K_0 is the attenuation of the stainless steel cable carrying the signal to the TLU. The second term on the right hand side of Eq. 4 had to be included due to the high attenuation figures of the stainless steel coaxial cable together with the high noise temperature of the warm amplifier.

A plot of the calibration data for the cold amplifier provided by the manufacturer can be seen in figure 9.

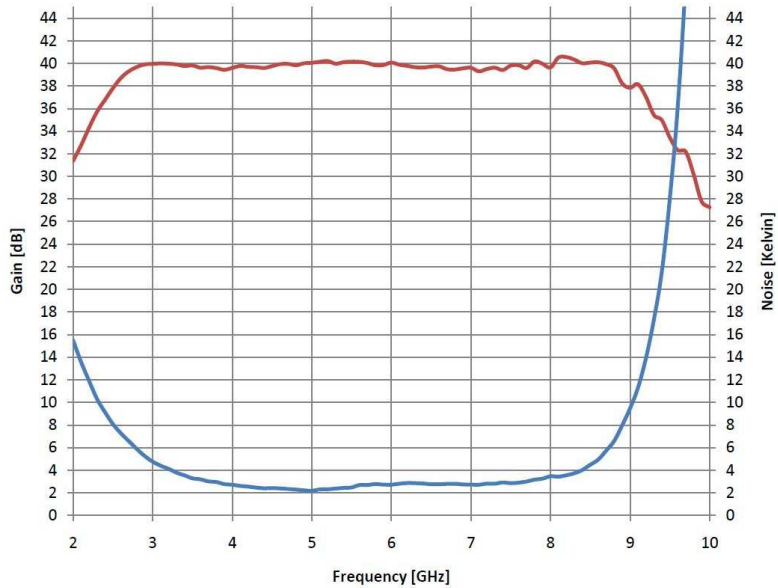


Figure 9: **Noise and Amplification Figures for Cold Amplifier.** Calibration results for the cold amplifier as stated on the specifications sheet provided by the manufacturer at 9.6K (where red corresponds to amplification figure and blue to noise temperature). It can be seen that the amplification figure is not exactly 40dB throughout the entire bandwidth.

5.2 Results

In order to measure the noise temperature of the cold amplifier, the previously mentioned Y-factor measurement scheme was used over the range of frequencies from 3GHz to 8GHz in steps of 0.5GHz, this frequency interval corresponds to the bandwidth of the cold amplifier. As a representative sample for each of our frequencies we considered data within a span of 10Mhz around each of the selected frequencies. For each of the frequencies enough time (5-10 mins) was allowed so that the spectrum analyzer could perform 25 averages at each frequency point. In addition, a moving average with a 100 point window was used.

Even though the measurements were originally planned to take place at 3K (cold stage) and 6K (warm stage), the temperature curve in figure 10 shows clearly that the temperature of our set-up increased as the cold amplifier was turned on (time indicated by the left-most red dot), hence providing an additional uncertainty factor for these measurements. Since no temperature sensor was directly mounted on the cold amplifier, precise knowledge of its

physical temperature was not possible.

The results for the power measurement can be seen in figure 11, and the corresponding noise temperatures can be seen in figure 12. The data points in figure 12 correspond to the noise temperatures calculated by means of Eq.4.

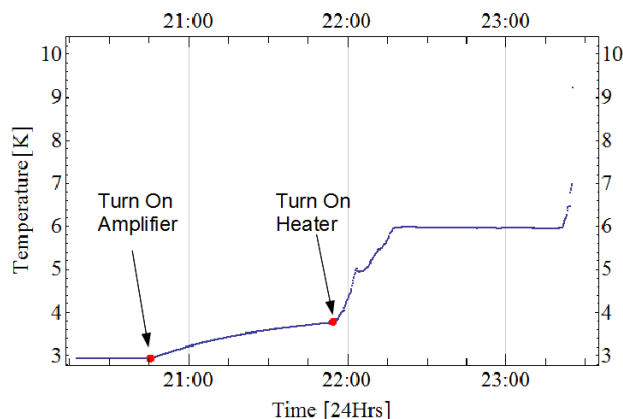


Figure 10: **Temperature of TNS.** The first red dot indicates the moment at which the cold amplifier was turned on, while the second one indicates the moment at which the heater is used to bring the temperature of the TNS up to 6K. It is clear that the physical temperature of the TNS was affected by the operation of the cold amplifier. Higher stability is observed at 6K, indicating that the physical temperature of the cold amplifier was below this temperature.

Error bars¹ can be seen to be of the order of 1K for most measurements. These results show noise temperatures 1.5-2K higher than those reported on the specifications sheet of the cold amplifier for a physical temperature of 9.6K; whether this is a product of a real increment in noise temperature as the temperature is decreased below that of the calibration is unknown yet unlikely since it seems reasonable to assume that a decrease in physical temperature will also lead to a decrease in noise temperature. These error bars are actually a lower bound on the true error values, since no uncertainty coming from the noise temperature, the amplification of the first warm amplifier as well as the amplification of the cold amplifier was available.

¹See section 5.3 for a discussion of the error bars.

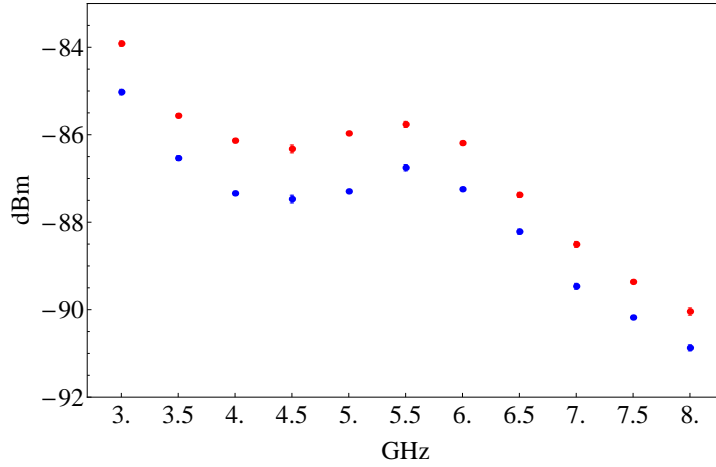


Figure 11: **Power Spectrum Measurements.** The data points shown here correspond to the power measured at frequency points between 3GHz and 8GHz. It can be seen that for higher frequencies their separation decreases very slightly, this is due to the fact that as the measurement was being performed the physical temperature of the cold amplifier was increasing, hence bringing the 'cold' measurements (blue) closer to the 'warm' measurements (red).

Finally one could ask whether the heating of the TNS right after the cold amplifier is operated could be the product of radiative heating instead of heat conduction through the cable. After comparing the orders of magnitude of the heat flow through the coaxial cable to an upper bound on the radiative mechanism, one comes to the conclusion that the latter is four orders of magnitude lower than the former, ruling out this possibility.

5.3 Error Bars

The error bars were obtained by means of the expression

$$\Delta T_c = \left[\frac{(T^\downarrow(Y-1) + (T^\uparrow - YT^\downarrow))Y \ln 10}{10(Y-1)^2} \right] \left((\Delta P^\uparrow)^2 + (\Delta P^\downarrow)^2 \right)^{1/2}$$

where ΔP^\uparrow and ΔP^\downarrow are the standard deviations of the spectral power measurements given in *dBm*, and as mentioned before no additional contributions, besides these, were taken

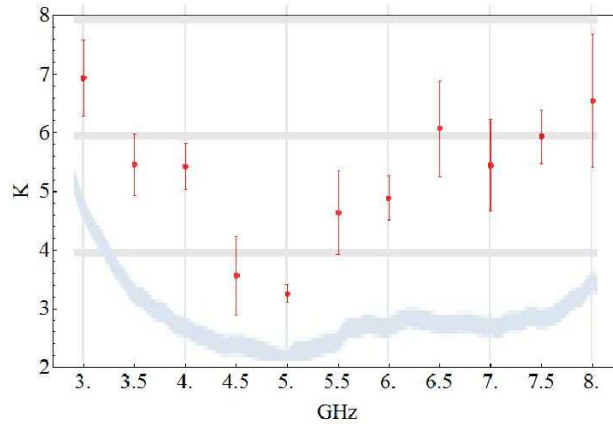


Figure 12: **Noise Temperature.** *Noise Temperature vs Frequency plot (red points) for the cold amplifier. A scaled image of the manufacturer's data is shown on the background (blue curve). Even though the shape of the measured data seems to reproduce the curve given in the specifications sheet, systematically higher noise temperature values were found throughout the entire bandwidth.*

into account. However, it can be seen that the contributions from uncertainties of the TNS temperatures can be quite significant since for an uncertainty of 1K in the temperature of the TNS, the contribution that one gets is of the same order of magnitude as the calculated noise temperature itself (see Mathematica notebook in[5]). For uncertainties of the gain of the cold amplifier, it turns out that they are slightly less relevant when compared to those stemming from the TNS temperature, the former being on the order of 0.1K for an uncertainty of 1dB.

It is clear from the measured data that systematic errors were present during the measurement, some of which (see discussion in conclusions) may have come from a lower temperature on the tip of the 50Ω termination or a higher than expected attenuation of the signal coming from the TNS, thus effectively providing a lower radiative contribution than expected and inducing a higher estimate for the noise temperature of the amplifier.

6 Conclusions

- As mentioned before, it is not entirely clear whether choosing stainless steel for the coaxial cable carrying the signal from the cold amplifier to the first warm amplifier had a significant effect on the quality of the signal read out. In principle, replacing this cable by a copper cable should reduce the attenuation figures significantly, keeping the noise introduced by the first warm amplifier out of the measurement and allowing for a “cleaner” measurement of the signal coming from the cold amplifier, this of course at the cost of a higher heat load on the set up.
- It was observed that the thermal insulation properties for the superconducting cable may have been overestimated given the fact that turning on the cold amplifier had an immediate effect on the physical temperature of the TNS. Thus, mounting an additional temperature sensor directly on the cold amplifier would be of use to gain additional understanding on the behavior, as well as the thermal properties, of the NbTi cable.
- An issue that could have had a systematic effect in our approach is the fact that we only used a heater, so that the temperature distribution was likely to have been inhomogeneous over the volume of the TNS, thus introducing an additional uncertainty factor since the tip of the 50Ω termination may have been at a different temperature from the one recorded at the temperature sensor.

Given that for the case of a parametric amplifier one would be working on a quantum-limited regime for the noise figures measured, and noting the contributions from uncertainties in physical temperature mentioned in section 5.3, it is of critical importance to arrive at a solution that provides a very high stability as well as certainty on the physical temperature of the TNS.

- An alternative approach to our calibration scheme can be found in an article by Castellanos-Beltran [8], where two different noise sources are used and fixed at different places in the cryostat. This may be a viable alternative in terms of providing

a higher thermal stability for the TNS and could also give a higher confidence on the temperatures at which the TNS are fixed, at the cost of introducing additional uncertainty into our measurement emerging from the fact that we would then need two different transmission lines carrying the signal from each TNS to the amplifier, each of which would contribute different attenuation figures as well as insertion losses. Along with the additional transmission line required, one would also need some switching device, e.g. a magnetic switch, allowing one to control which TNS effectively radiates on the amplifier, which would in turn also contribute an insertion loss thus providing an additional source for uncertainty.

- It remains to test the performance of this approach at lower temperatures, particularly at temperatures close to that of the base plate, since it is to be expected that at such low temperatures the inclusion of a heating element on the coldest stage, such as the TNS, in conjunction with a lower-than-expected performance by the NbTi cable may alter significantly the operational temperature of the set-up.

References

- [1] Pozar D., *Microwave Engineering*, Wiley John + Sons, 2004.
- [2] Q:\USERS\Juan\Semester Project\Data Sheets & Sketches.
- [3] Q:\USERS\Juan\Semester Project\Photos.
- [4] Q:\USERS\Juan\Semester Project\Literature on Parametric amplifier.
- [5] Q:\USERS\Juan\Semester Project\Mathematica Notebooks\Noise Measurements.
- [6] Q:\USERS\Juan\Semester Project\Mathematica Notebooks\Heat Transfer Simulations.
- [7] Q:\USERS\Juan\Semester Project\Thermal Properties of Materials.
- [8] Castellanos-Beltran M.A. *et al.* Amplification and squeezing of quantum noise with a tunable Josephson metamaterial. *Nature Phys.* **4**, 928-931 (2008).